Understanding the Formation of Geopolymer Foams: Influence of the Additives

M. Arnoult [a,b], M. Perronnet [b], A. Autef [b], B. Nait-Ali [a], S. Rossignol [a]*

[a]Univ. Limoges, IRCER, UMR 7315, Limoges, France; [b]Imerys Ceramics, Imerys Ceramic Centre, Limoges, France

Geopolymer foams are innovative materials synthetized at low temperature, resulting from the activation of an aluminosilicate source with an alkaline solution. The purpose of this study is to understand the role of additives, such as surfactants and fillers, on foam formation. Four different geopolymer foams were synthetized and analyses on their microstructure, density, mechanical resistance and thermal conductivity were carried out. Then, the reactive mixtures of dense geopolymers were studied by the means of FTIR, viscosity and surface tension measurements. The addition of surfactants leads to an increase in the volume expansion up to 4.03, in the porosity rate with a homogeneous microstructure and therefore the foam thermal conductivity and the compressive strength decrease to 57 mW/m.K and from 4950 to 52 kPa respectively. Besides, it modifies the polycondensation reaction by delaying the beginning of the reaction by up to 80 minutes. However, it appears the addition of silica fibers does not impact the geopolymer formation and improves the mechanical properties by 70%. This study also reveals that the ratio of surfactant (300) to metakaolin is crucial in order to stabilize the wet foam before its consolidation.

Keywords: Geopolymer, Foam Formation, Surface Tension, Viscosity, Thermal Conductivity.

1. Introduction

Nowadays, the building industry is one of the largest energy consumer as well as a major greenhouse gases emitter. Therefore, the development of materials requiring less energy and/or emitting less CO_2 during their production and that can permit to reduce the energy expended is an ongoing challenge. Besides, in housing applications, there is a real interest in substituting organic products by inorganic ones in order to increase their fire resistance. In this context, thanks to their low heat conductivity [1, 2], good heat resistance [3] and acoustic properties [4], mineral foams are expected to be an interesting alternative for the building industry. Mineral foams can be synthetized by chemical or mechanical introduction of a gas into a liquid phase [5]. Thus, the mineral foam is at first a dispersion of gas bubbles in a continuous liquid phase, which is a thermodynamically unstable system evolving irreversibly [6]. Various phenomena, such as coarsening, drainage [7] or coalescence [8], can occur during the aging of the foam, increasing the bubbles' size over time, which can be the cause of a phase separation between the liquid and the gas [9, 10]. Therefore, during the mineral foam formation, there is a critical step where it exists as a liquid foam, which it is essential to stabilize in order to control the architecture of the final consolidated foam. In general, synthetizing foams requires the presence of surfactant molecules [11], which are usually composed of a polar (hydrophilic) head group and a non-polar (hydrophobic) chain tail [12]. The surfactant preferentially adsorb at the air/water interface, thus reducing the free energy involved by increasing the surface area of the interface. As a result, it reduces the interfacial surface tension [13]. From the moment the surface is saturated, the surface tension remains constant. This change in behavior [14, 15] is linked to the critical micelle concentration (CMC) [16], which allows to determine the surfactant concentration necessary for its effective utilization [17].

Two major parameters have an influence on the liquid foam stabilization and can even slow it down: the surface tension and the viscosity [6, 18]. Therefore, it is crucial to use a surfactant to decrease the surface tension, but also an additive (such as fillers, charge etc.) to modify the viscosity in order to decrease the drainage rate, as demonstrated by Safouane et al., using glycerol as the additive [19]. Moreover, numerous studies highlighted the influence of the addition of solid particles on drainage and coalescence, and thus on the foam stabilization [20, 21, 22]. It actually increases the mixture's viscosity and thus improves the resistance to coalescence. Besides, Ottewill et al., showed the impact of solid particles on viscosity by decreasing the drainage [23], and Alargova et al. studied the influence of the particles' shape on the foam stability [24]. Indeed, non-spherical particles can be oriented differently at the air/liquid interface, thus modifying the network and therefore the foam stability.

Among the exisiting foams, geopolymer foams are expected to be used in many technological applications thanks to their properties. Numerous papers highlighted the fact that they present a real interest for thermal insulation applications [1, 2, 25]. Nevertheless, the control of the porosity dimension is still not well understood. It is established that geopolymers, obtained by the activation of an aluminosilicate source with an alkaline solution [26], are synthetized at room temperature. Then, the polycondensation reactions provide an amorphous three-dimension geopolymer network [3, 27]. However, numerous studies have demonstrated that geopolymer foams can also be synthetized in the same conditions with the in-situ formation of the pores. Prud'homme et

al. [28, 29] highlighted the possibility to produce geopolymer foams with the introduction of silica fume.

The influence of different parameters on the foams' properties was studied, such as the type and amount of foaming agent used or the curing conditions. However, few studies are focused on the effect of additives on the geopolymer mixture and therefore on the liquid foam stabilization. Indeed, in this type of materials, both the pore dispersion and the geopolymer mixture evolving over time may represent a challenge for their production. The aim of this work is to understand the geopolymer foams' formation before its consolidation. Thus, the synthesis and characterization (density, mechanical resistance and thermal conductivity) of four different geopolymer foams were carried out. Finally, the reactive mixtures of dense geopolymers were investigated by FTIR, viscosity and surface tension measurements in order to highlight the relation between these mixtures and the geopolymer foams' properties.

2. Experimental Part

2.1. Raw materials and sample preparation

Geopolymer foams were synthetized using an alkaline silicate solution ($S_{1.Na}$), a metakaolin (M_K) supplied by AGS and a foaming agent. Moreover, sodium hydroxide pellets were dissolved into the starting solution to adjust the Si/M ratio at 0.58. As a filler, silica fibers (SF) or/and a nonionic surfactant (T) can be added to the reactive mixture to optimize the foam stability (Table 1). The foams were obtained following the procedure presented in Fig. 1., and the resulting mixture was placed in a closed and sealed polystyrene mold at 40 °C. Four formulations were studied, only differenciated by the nature of the additives introduced into the geopolymer mixtures. Those geopolymer foams or reactive mixtures are represented as $^{T(y)}S_{1.Na}M_{K(x)SF}$, with T marking the samples with surfactant, y the amount of surfactant introduced, $S_{1.Na}$ the silicate solution adjusted at 0.58, M_K the metakaolin, x the amount of metakaolin added and SF marking the presence of silica fibers. As an example, $^{T}S_{1.Na}M_{K.SF}$ refers to the geopolymer foam obtained with the addition of silica fibers and surfactant.

2.2. Technical characterization

XRD patterns were recorded with a Bruker D8 Advance diffractometer using the CuK_α radiation. The acquisitions were done with a 5° to 45° 2θ-angle variation, a step size of 0.02° and an equivalent measured time per step of 50 s. The analyses of the XRD patterns were carried out using the powder diffraction file (PDF) database of the International Center for Diffraction Data to identify the different crystalline phases in the samples. The deconvolutions of the amorphous domes observed in the sample were performed using the Peakoc software [30]. The refinement was done between 5° and 45 ° using a Voigt function that takes into account the $K_{\alpha1}$ and $K_{\alpha2}$ radiations, and the continuous background was fitted with a second-degree polynomial.

Fourier-transform infrared (FTIR) spectroscopy in ATR mode was used to investigate the reactive mixture and the structural evolution of the geopolymer foam mixtures. The FTIR spectra were obtained using a ThermoFisher Scientific Nicolet 380 infrared spectrometer and were collected over a 400 to 4000 cm⁻¹ range with a 4 cm⁻¹ resolution. The atmospheric CO_2 contribution was replaced by a straight line between 2400 and 2280 cm⁻¹. To monitor the geopolymer formation, a spectrum (64 scans) was automatically recorded every 10 min for 13 h.

Table 1. Nomenclature and composition of the different raw materials used in the synthesis of geopolymer foams.

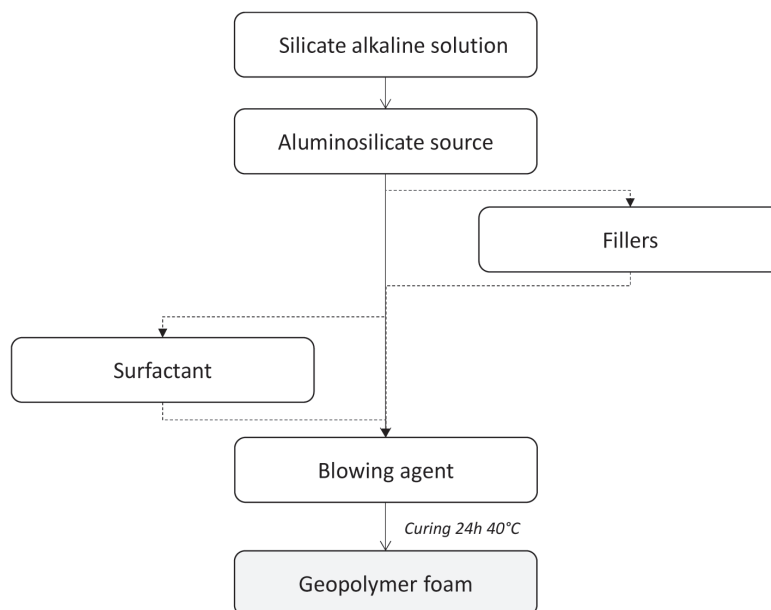| Raw materials	Name	Nomenclature	Composition
Alkaline silicate solution	/	$S_{1.Na}$	Si/M = 0.58
Aluminosilicate source	Metakaolin	M_K	Si/Al = 0.98
Blowing agent	Metal powder	/	Purity = 99 wt%
Additives	Silica Fillers Surfactant	SF T	65 < SiO_2 < 75% /

Figure 1. Synthesis protocol of the geopolymer foam samples.

For ease of comparison, the spectra were baseline-corrected and normalized [31].

A Brookfield DV-II was used to measure the evolution of the viscosity over time at given shear rates. Those measurements were performed during the geopolymer formation on 60 mL-samples of the reactive mixtures in a cylindrical container. The viscosity values were calculated by taking the average over one-minute measurements. The spindles were chosen depending on the mixture's viscosity and their speed varies from 100 rpm for low-viscous to 0.1 rpm for high-viscous mixture. The setting time of each geopolymer mixture was determined based on the intersection of the two tangents to the regimes seen on the viscosity curve.

The surface tension measurements were carried out on a Digidrop MCAT from GBX, comprising a camera and a lamp allowing to record the image drop. Those measurements were performed on 2μL-droplets of geopolymer mixture at room temperature with teflon-coated needles. The software Visiodrop (GBX) in the Young Laplace mode was used to record the surface tension. This device cannot be used with solid particles because it cannot pass through the needle.

The morphology and structure of the foam samples were observed using a FEI Quanta 450 FED scanning electron microscope (SEM) at 10 kV. A piece of geopolymer was slightly rubbed down to obtain an optimal surface, then placed on a carbon plate and coated (30 sec) with a Pt-Ag deposit.

The foam's volume expansion (Ev) is defined as the ratio of the foam volume after consolidation to the initial volume of mixture

introduced in a cylinder mold. This volume expansion was directly measured after 24h in a 40 °C oven.

The thermal properties of the samples were determined using the "hot disk" method performed using the Hot disk TPS 1500 with a 6.403 radius and placing the sensor between two elements of the same sample. The measurements were repeated 3 times per sample, keeping the mean value in the end.

Finally, the compressive strengths of the geopolymer foam samples were evaluated using a LLOYD EZ20 universal testing machine with a 0.5mm/min crosshead speed, carrying out two tests for each formulation. The samples, of a 27 mm diameter and a height of approximately 56 mm, were aged for 7 days.

All the samples were characterized after a drying step at 25 °C (60%HR) until the water loss remains stable.
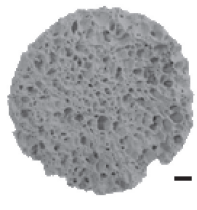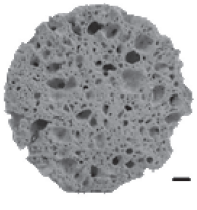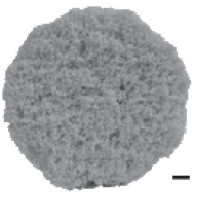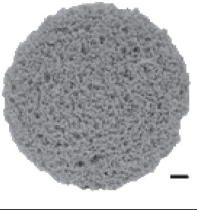
3. Results

3.1. Foam physical properties

The physical characteristics of the geopolymer foams are reported in Table 2. The reference foam has a density value of 0.40 g.cm^{-3}, a thermal conductivity of 0.099 W.m^{-1}.K^{-1} and a compressive strength of 1540 kPa. In order to improve the foam's stability and its mechanical strength, fillers were added to the original formulation [21]. This addition of silica fibers leads to a 27% increase in density (0.40 and 0.55 g.cm^{-3} for $S_{1.Na}M_K$ and $S_{1.Na}M_{K.SF}$ respectively) and another 70% increase in the compressive strength, without impacting the thermal conductivity. Besides, adding silica fibers also sees a decrease in the foam's volume expansion (Ev) from 1.61 to 1.53.

On the other hand, the two samples synthetized with surfactant show lower densities and thermal conductivities, as well as a higher volume expansion. Thus, the presence of surfactant induces a decrease in the thermal conductivity from 0.099 to 0.058 mW.m^{-1}.K^{-1} for $S_{1.Na}M_K$ and $^TS_{1.Na}M_K$ respectively. Moreover, the compressive strength of these materials strongly drops (from 4950 to 52 kPa for $S_{1.Na}M_{K.SF}$ and $^TS_{1.Na}M_{K.SF}$). Besides, these samples present a more homogenous pore distribution. This phenomenon can be explained by a better foam stabilization.

The different variations of the compressive strength as a function of strain are displayed in Fig. 2. It is to be noted that the mechanical properties of $^TS_{1.Na}M_K$ could not be measured due to their fragility. Three different behaviors can be observed. The evolutions of $S_{1.Na}M_K$ and $S_{1.Na}M_{K.SF}$ present a linear component typical of an elastic regime, followed by a slight plastic deformation and a brittle failure. Otherwise, $^TS_{1.Na}M_{K.SF}$'s evolution shows a rise in the compressive strength as the strain increases, but no fracture is noticed. Then, after the strain reaches 6%, the compressive strength only presents a slight increase. In the case of no fracture, let it be noted that the final compressive strength registered is the one collected for 10% of strain. These different behaviors can be explained by the porosity rate of the microstructure, a rise in the porosity rate leading to a decrease in the compressive strength [32].

In order to analyse their microstructure, SEM micrographs of the geopolymer foams are gathered in Fig. 3. The samples exhibit different behaviors in terms of microstructure and porosity. Incidentally, the four samples studied show different pore shapes and sizes. $S_{1.Na}M_K$ presents a heterogeneous pore size

Table 2. Physical and chemical features of the synthesized geopolymer foams.

Samples	Pictures	ρ (g/cm³)	E$_v$	Thermal conductivity (W.m^{-1}.K^{-1})	Compressive strength (kPa)
$S_{1.Na}M_K$		0.400	1.61	0.099	1540
$S_{1.Na}M_{K.SF}$		0.550	1.53	0.100	4950
$^TS_{1.Na}M_{K.}$		0.130	3.84	0.058	< 50
$^TS_{1.Na}M_{K.SF}$		0.136	4.03	0.057	52
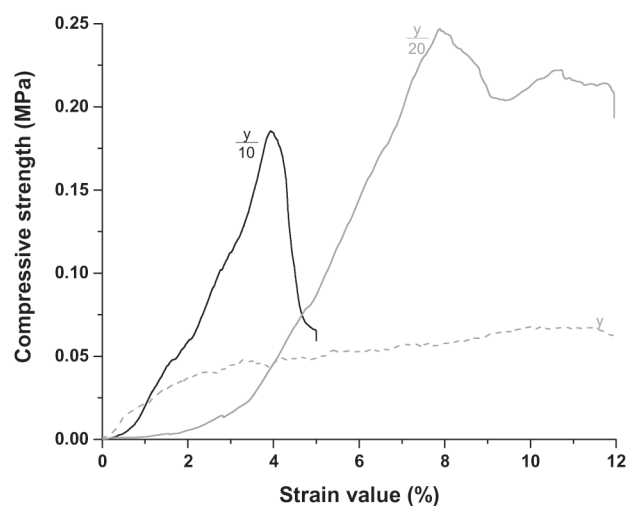
Figure 2. Compressive strength value as a function of the strain value for $S_{1.Na}M_K$/10 (—), $S_{1.Na}M_{K.SF}$/20 (—), and $TS_{1.Na}M_{K.SF}$ (- -) samples (Y/20=Compressive strength value divided by 20).

distribution confirming the coalescence phenomenon [7, 8]. $S_{1.Na}M_{K.SF}$ also shows heterogeneity in term of pore size and the silica fibers are randomly oriented. In this case, it appears that the coalescence phenomenon occurs before the foam consolidation. With the addition of surfactant, the characteristics of the foam are completely different, $TS_{1.Na}M_K$ presenting a homogeneous

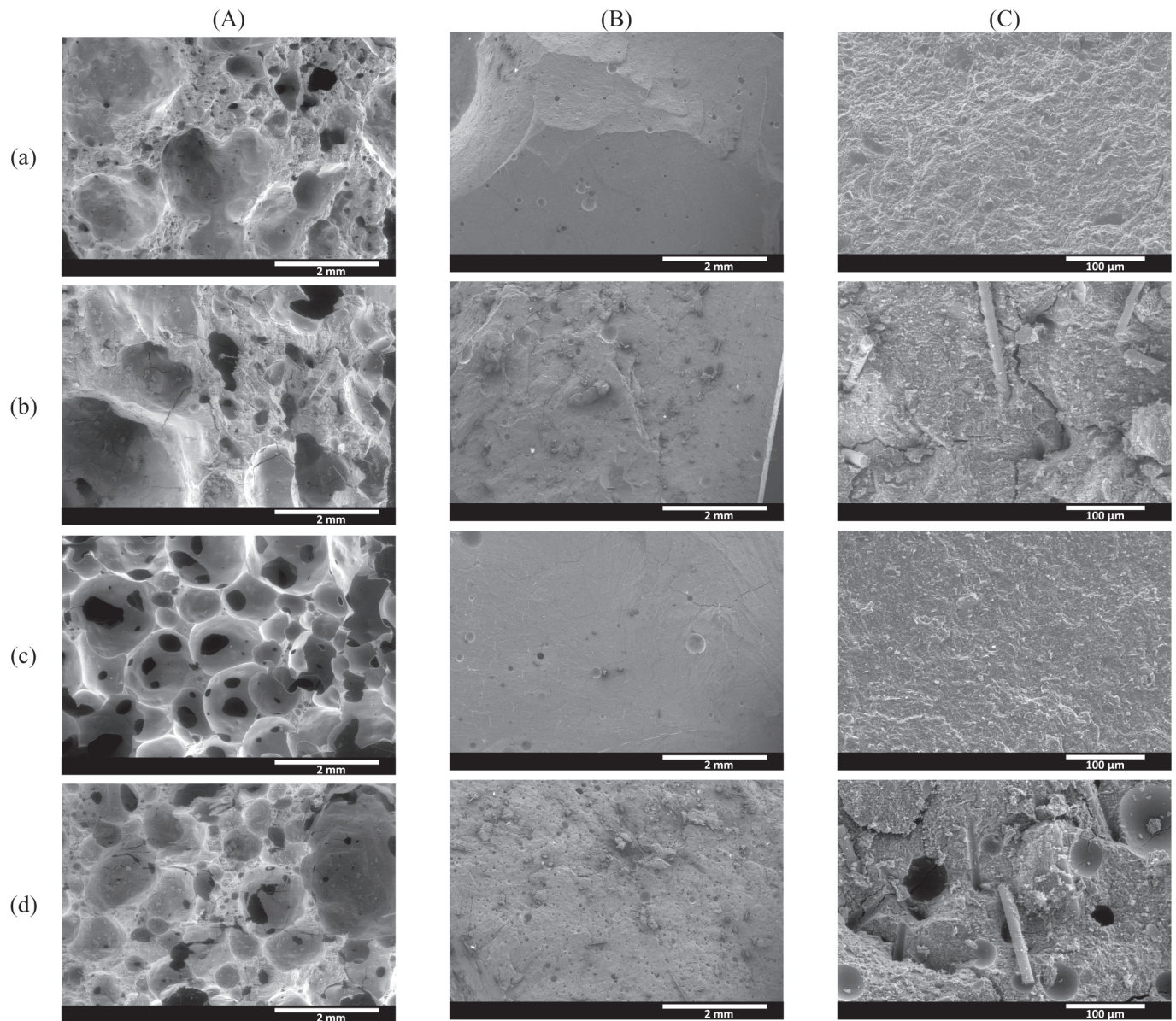(A)   (B)   (C)

Figure 3. SEM micrographs of foam (A), dense X80 (B) and dense X300 (C) for the following geopolymer samples: (a) $S_{1.Na}M_K$, (b) $S_{1.Na}M_{K.SF}$, (c) $^{TS}_{1.Na}M_K$ and (d) $^{TS}_{1.Na}M_{K.SF}$.

pore size distribution. Moreover, this pore size augments and all pores are interconnected, which suggests that the coarsening phenomenon occurs before the foam consolidation [7]. $TS_{1.Na}M_{K.SF}$ also presents both a more homogenous pore size distribution and randomly oriented silica fibers. Therefore, these features changes are probably due to the liquid mixture stability and to the liquid-air interface, which can be modulated by the viscosity and the surface tension. This point will be further discussed.

The XRD diffractograms are presented in Fig. 4. MK's XRD pattern (Fig. 4.e) displays a broad peak typical of an amorphous material as well as peaks relative to crystalline phases such as quartz and anatase. In the case of crushed geopolymer samples (Fig. 4.a', b', c', d'), the displacement of the amorphous dome pinpoints the metakaolin's dissolution and the formation of a geopolymer network based on SiO_4 and AlO_4 tetrahedra [33]. Besides, the crystalline phases in the metakaolin are also observed in the crushed samples, which can be explained by the fact that they were not altered. The same tendency is observed in the geopolymer foam (Fig. 4.a', b', c', d'). Nevertheless, the network formed seems to be different.

The different positions of the domes for each sample (geopolymer foams and binders) were determined with the protocol explained in part 2.2. Fig. 5 A presents an example of a deconvoluted

diffractogram of a $S_{1.Na}M_K$ dense geopolymer. For all samples, two contributions centered around 22 and 29° (main dome) can be observed. The later is a characteristic of geopolymer materials and outlines the complete alteration and consumption of the metakaolin [34]. The former (22°) proves the presence of a SiO_2 amorphous network (Si-O short order structure) [35, 36]. This phenomenon can be explained by the excess of potassium silicate solution that can induce the formation of SiO_2 based network due to a metakaolin deficiency.

Fig. 5 B presents the evolution of the dome positions for the different samples. The domes of $S_{1.Na.}M_K$ (dense geopolymer) are centered at 22.04° and 29.11°. The same behavior is observed for geopolymer foams and geopolymer binders. Thus, the dome at around 29° doesn't shift whatever the additives introduced. On the contrary, the dome at around 22° shifts depending on the additives introduced, which shows the formation of a disordered network [37]. The fillers (silica fibers) being of amorphous nature [38], they induce the shift of the dome to higher 2θ°: 22.04° and 22.28° for $S_{1.Na}M_K$ and $S_{1.Na}M_{K.SF}$ respectively. On the other hand, the addition of the surfactant causes a displacement from 22.04 to 22.37° due to the disorder induced [37]. The difference observed between the dense geopolymer and the geopolymer foams at the dome position centered around 22° is related to the disorder
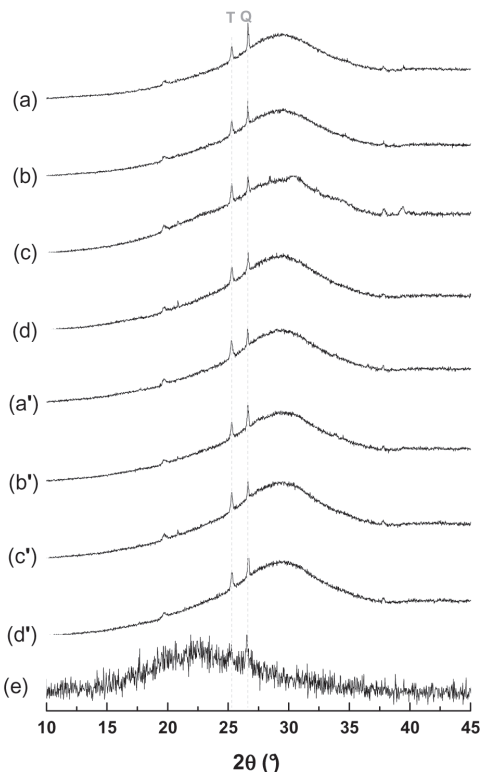
Figure 4. XRD patterns of the geopolymer foams (a) $S_{1.Na.}M_K$, (b) $S_{1.Na.}M_{K.SF}$, (c) $^TS_{1.Na.}M_K$, and (d) $^TS_{1.Na.}M_{K.SF}$, of the dense geopolymers (a') $S_{1.Na.}M_K$, (b') $S_{1.Na.}M_{K.SF}$, (c') $^TS_{1.Na.}M_K$, and (d') $^TS_{1.Na.}M_{K.SF}$, and of the metakaolin M_K (e) (PDF files: Q: Quartz (01-086-1630); T: Titanium oxide (01-071-1167)).

introduced by the chemical foaming created by the foaming agent [39] due to the weak amount of Si and Al atoms.

3.2. Reactive mixtures

Further investigation is necessary to understand the foam formation by isolating the influence of each additive during the process, thus the necessity to study the geopolymer mixture. However, the gas released limits the viscosity measurements, which are then not effective in this case. Therefore, the geopolymer mixture without the blowing agent was studied.

FTIR spectroscopy data

In order to assess the influence of the additives (silica fibers and surfactant) on the polycondensation, the structural evolution of the synthesized mixture was monitored using FTIR spectroscopy in ATR mode on the various formulations. Fig. 6. A presents an example of infrared spectra recorded at different recording times (t=0; 200 and 400 minutes) for $S_{1.Na}M_K$. The measurements were carried out for 350 minutes because the sample does not coat the diamond after that mark, and consequently the acquisition cannot be finished. Due to this measurement limit, only the beginning of the reaction was recorded. At t=0 min, three contributions can be isolated: two at 3255 cm^{-1} and 1620 cm^{-1} attributed to υ_{OH} and δ_{OH} respectively, and one at 1000 cm^{-1} assigned to the Si-O-M (Q^2) contribution. Moreover, with time, two phenomena can be observed. First, the decrease of the H$_2$O band intensity and second, the shift of the Si-O-Si band towards lower wavenumbers, which is typical of the polycondensation reaction. To compare the different geopolymer mixtures,
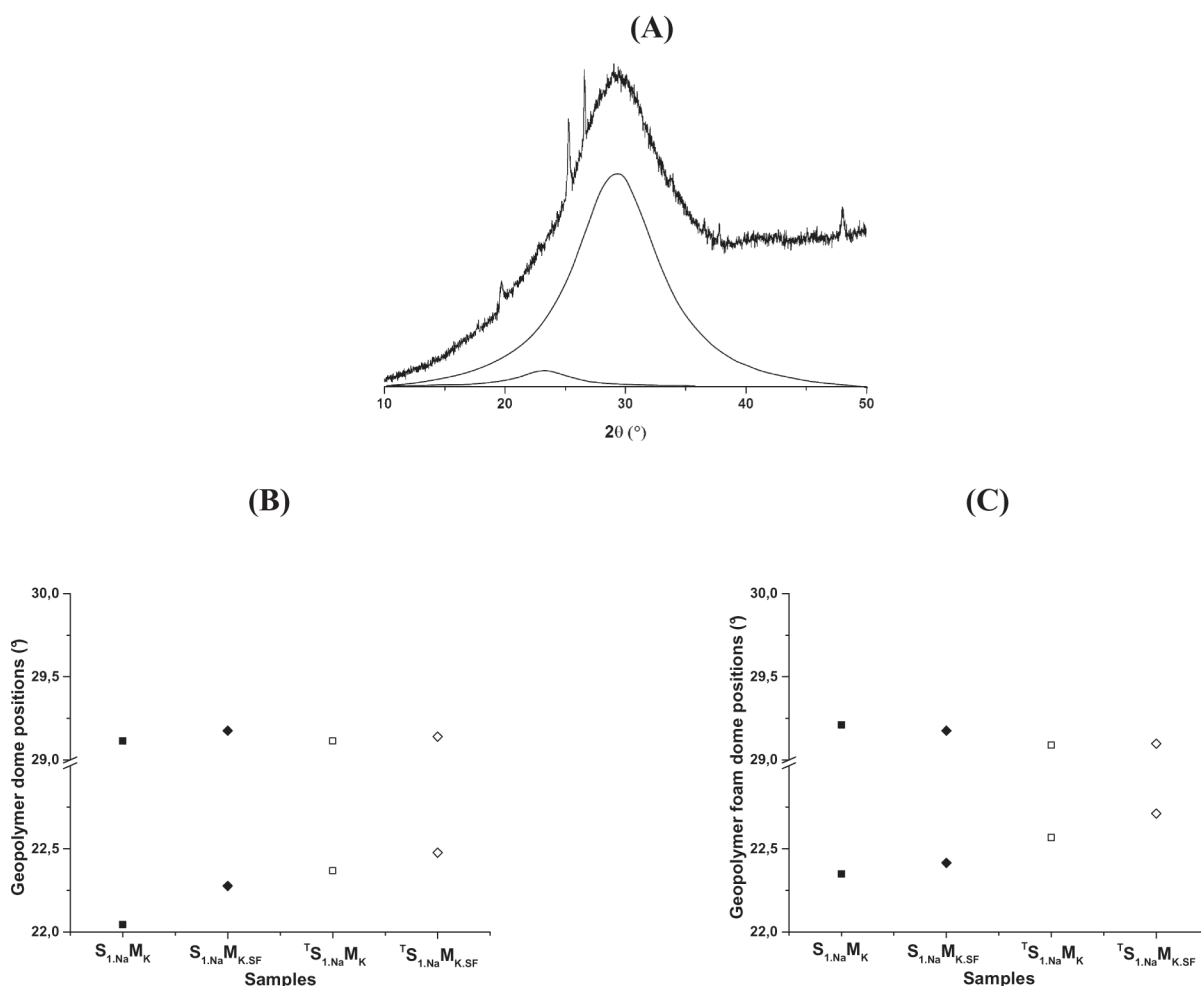
(A)

(B)

(C)

Figure 5. (A) Examples of the deconvoluted diffractogram of the dense geopolymer $S_{1.Na.}M_K$ and of the evolution of the various broad peaks (22° and 29°) locations values (± 0.001) for the different formulations of (B) dense geopolymers and (C) foams: (■)$S_{1.Na.}M_K$, (□)$^TS_{1.Na.}M_K$, (♦)$S_{1.Na.}M_{K.SF}$, and (◊)$^TS_{1.Na.}M_{K.SF}$.

(A)

(B)

(C)

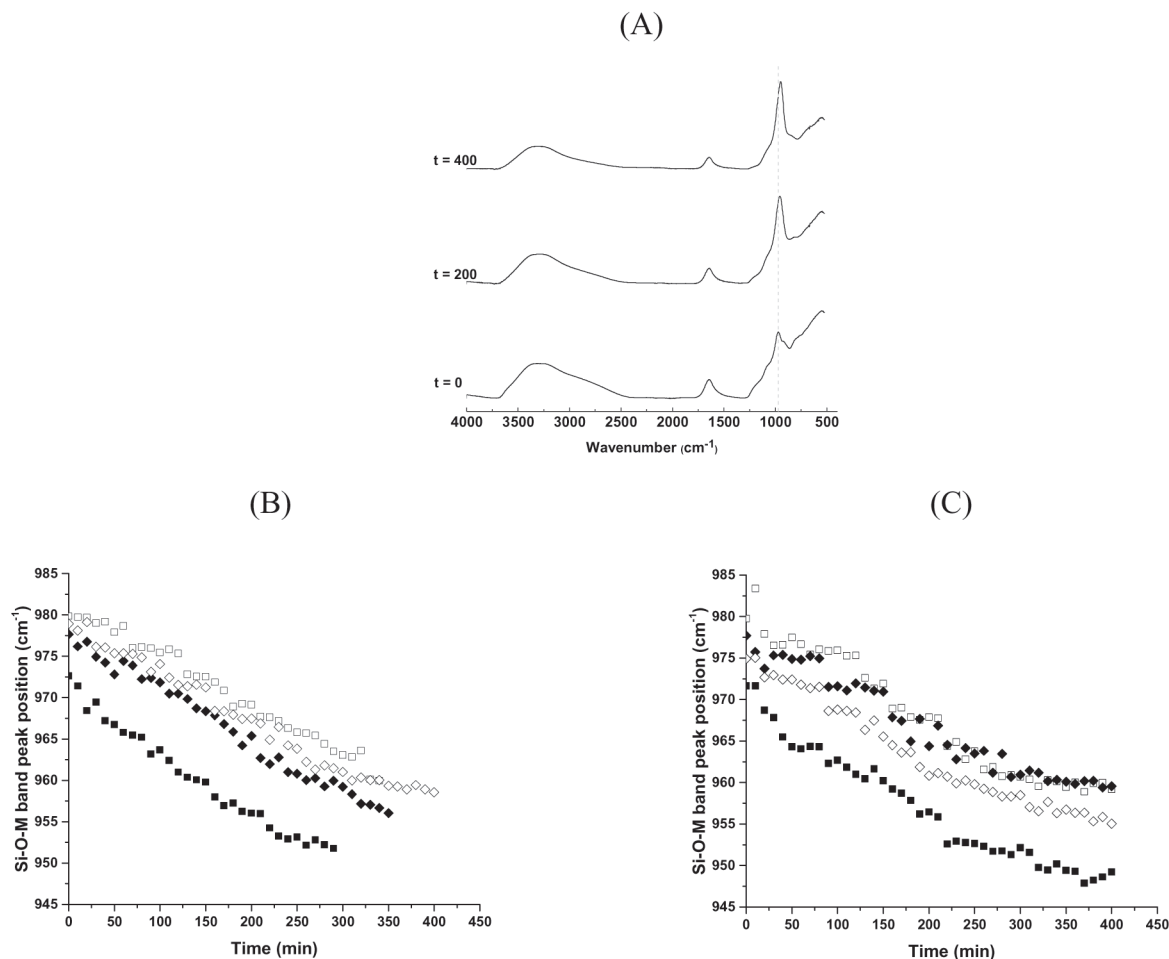*Figure 6. (A) Example of FTIR spectra recorded at t=0, 200 and t=400 min for $S_{1.Na.}M_K$, and evolution of the shift of the Si-O-M band (± 4 cm-1) as a function ot time for (B) dense geopolymers and (C) foams: (■)$S_{1.Na.}M_K$, (□)$^TS_{1.Na.}M_K$, (♦)$S_{1.Na.}M_{K.SF}$, and (◊)$^TS_{1.Na.}M_{K.SF}$.*

Fig. 6 B, C show the Si-O-M shifts towards lower wavenumbers for mixtures without and with foaming agent respectively. This shift underlines the substitution of Si-O-Si bonds by Si-O-Al, and thus reflects the polycondensation reactions [40, 41], with the curve's slope being specific for the kinetics of this substitution.

In the case of dense geopolymers (Fig. 6 B), the initial band of $S_{1.Na.}M_K$ (972 cm^{-1}) is lower than that of the other samples ($\approx$979 cm^{-1}) and this difference appears to be related to the additives (fillers and surfactant) introduced. As a matter of fact, the initial Si-O-M peak position is linked to the siliceous species and the number of non-bridging oxygen atoms (NBO) [42]. The addition of fillers changes the water demand of the mixture, decreasing the solution reactivity by modifying the diffusion of silicate species [43]. Concerning $^TS_{1.Na.}M_K$, the position of the Si-O-M peak is constant at 978 ± 4 cm^{-1} for 80 minutes. It appears the OH$^-$ groups of the surfactant can affect the dissolution processes [44], resulting in the delay of the polycondensation reaction. The same tendency is observed with $^TS_{1.Na.}M_{K.SF}$ where the OH$^-$ groups from the surfactant modify the beginning of the reaction. Regarding all samples, after 350 minutes, the shift values and the slopes are quasi similar. This very slight variation may be attributed to the presence of additives, thus implying that this addition does not have an influence on the geopolymer network formed. The addition also appears to slightly enhance the network reorganization without affecting the kinetics of the polycondensation reaction.

Fig. 6 C presents the same tendency in the case of geopolymer foams, including the initial band of $S_{1.Na.}M_K$ (973 cm^{-1}), still lower than the other samples' ($\approx$979 cm^{-1}). Unlike dense geopolymers, the addition of fillers or surfactants in geopolymer foams leads to the apparition of a longer delay relative to the Si-O-M peak position. This phenomenon can be explained by the higher

disorder of the reactive mixture caused by the fillers and the release of dihydrogen, inducing different aluminosilicate source dissolution steps [39]. However, the shift values after 350 minutes are similar to the dense geopolymers. Therefore, the dense and porous geopolymers exhibit the same network, suggesting that the oligomers formed are not modified. As a result, only a difference in the short range disorder was observed by XRD measurement. There is not much difference between reactive mixtures with or without foaming agents. Consequently, the end of this paper focuses on the analysis of reactive geopolymer mixtures without the addition of a foaming agent.

Reactive mixtures

It has been demonstrated in Fig. 3 that the pore size distribution and the microstructure are different depending on the additives used (surfactant, silica fibers). This phenomenon can be explained by the viscosity and the surface tension of the geopolymer reactive mixture.

Viscosity

The viscosity of each geopolymer mixture, based on the introduction of different additives (silica fibers and/or surfactant), was collected in order to analyse their influence on the geopolymer foam formation. These data were gathered in Fig. 7 where Fig. 7 A shows a representation of the different viscosities as a function of time. The same trend is observed, whatever the reactive mixture considered. Over time, a slow increase in viscosity is indeed seen, followed by a very strong increase after approximately 100 minutes, testifying of the geopolymer consolidation. Besides,
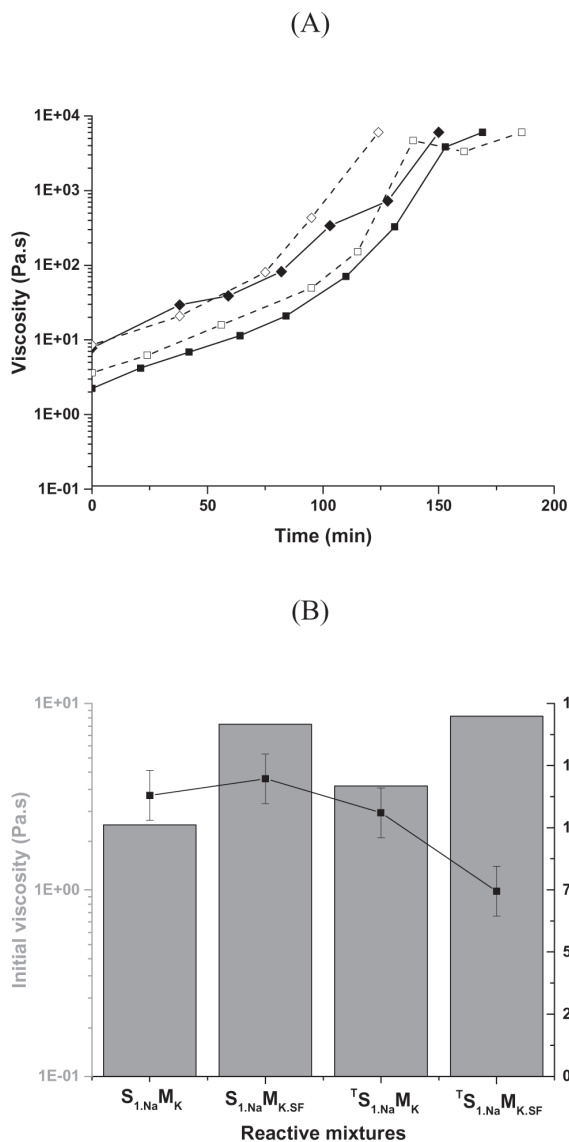
(A)

(B)

Figure 7. (A) Viscosity as a function of time for the reactive mixtures (■)$S_{1.Na}M_K$, (♦)$S_{1.Na}M_{K.SF}$, (□)$^TS_{1.Na}M_K$, and (◊)$^TS_{1.Na}M_{K.SF}$ and (B) their initial viscosity and setting time (precision ± 0.5 Pa.s).

(A)

(B)

Figure 8. Evolution of the surface tension value as a function of (A) the metakaolin content with the S1.Na solution and of (B) the surfactant concentration for (□)$S_{1.Na}$ (■)$S_{1.Na}M_{K(5g)}$ and (■)$S_{1.Na}M_{K(10g)}$.

Fig. 7 B presents the evolution of the initial viscosity and the setting time of the various geopolymer mixtures. Two trends are then observed: on one hand, the addition of silica fibers causes the initial viscosity value to rise and, on the other hand, the addition of surfactant seems to lower the setting time of the geopolymer mixture.

More precisely, the addition of silica fibers takes the initial viscosity from 2.23 to 7.73 Pa.s for $S_{1.Na}M_K$ and $S_{1.Na}M_{K.SF}$ respectively. Furthermore, with an increase in initial viscosity of 58% (from 3.61 to 8.53 Pa.s for $^TS_{1.Na}M_K$ and $^TS_{1.Na}M_{K.SF}$ respectively), the addition of silica fibers induces the same behavior for the formulations containing a surfactant. It is to be noted that the difference in initial viscosity can be explained by the water demand of the dry weight as well as the shape of the fillers. It has indeed been demonstrated that a fiber filler has a strong impact on the viscosity [45]. On the other hand, $S_{1.Na}M_K$ and $S_{1.Na}M_{K.SF}$ mixtures both have a setting time of approximately 115 minutes, implying that the addition of silica fibers does not influence the setting time.

The presence of a surfactant does not affect the initial viscosity of the reactive mixture, as only a small rise in viscosity is noticed (from 2.23 to 3.61 Pa.s for $S_{1.Na}M_K$ and $^TS_{1.Na}M_K$ respectively). Concerning the formulations with silica fibers, the same tendency is noted. In addition, the presence of both the surfactant and silica
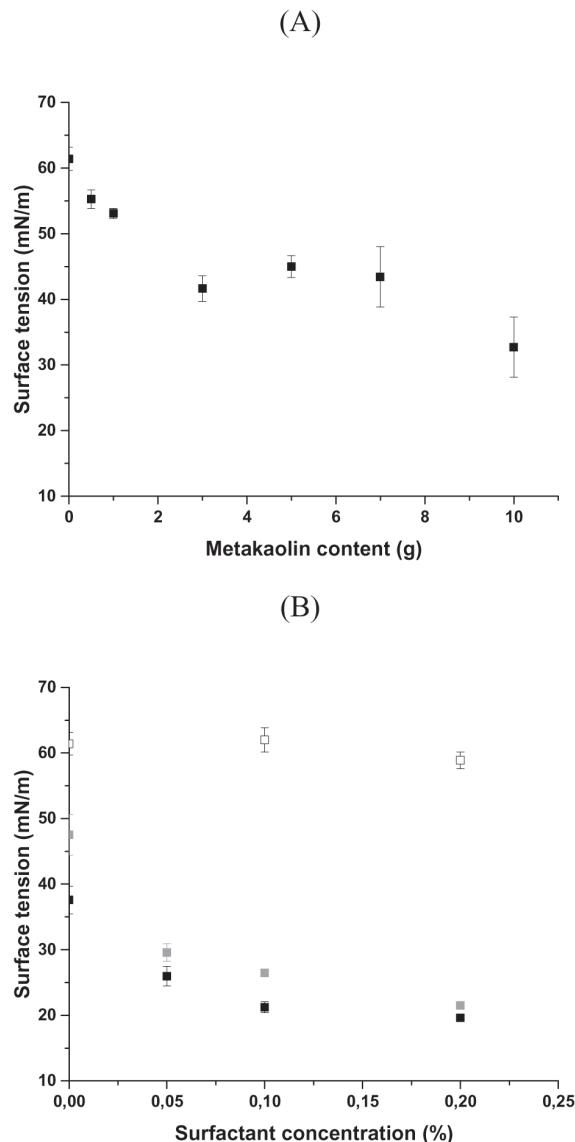
fibers results in a drop of the setting time by 38% (from 120 to 75 minutes for $S_{1.Na}M_{K.SF}$ and $^TS_{1.Na}M_{K.SF}$ respectively), thanks to the surfactant containing OH groups which tend to create anchor points enhancing the polycondensation reaction [46, 47].

Surface tension

The surface tension can be defined as the attractive force at the interface between two different media (liquid-oil or liquid-air). The knowledge of this property is crucial in order to comprehend the different interactions in the geopolymer mixtures as well as to optimize the foam stability [6, 18]. Fig. 8 regroups two variations of the surface tension as a function of the metakaolin (MK) mass added first (Fig. 8 A) and the surfactant concentration second (Fig. 8 B) for different geopolymer compositions.

Fig. 8 A shows the general trend that the more metakaolin is added in the alkaline silicate solution, the lower the surface tension is. Thus, if the initial surface tension of the alkaline silicate solution is around 61 mN.m^{-1}, the addition of 1g of metakaolin leads to a 14% decrease of this initial value (53 mN.m^{-1} for $S_{1.Na}M_{K(1)}$). Moreover, a surface tension of around 40 mN.m^{-1} is measured after adding 3 g of metakaolin, value which stays constant up to 8 g of MK added. As a matter of fact, with a low amount of aluminosilicate

source (3 to 8 g), the available metakaolin in the solution is too low for it to react with the silicate species from the alkaline silicate solution [48]. Then, with adding 9 g of metakaolin, the drop in surface tension resumes, reaching 32 mN.m^{-1} for $S_{1.Na}M_{K(10)}$. At this point, a sufficient amount of species from the metakaolin are then available in the solution, therefore the mixture is more reactive, these numerous interactions resulting in the decrease of the surface tension. Besides, let it be noted that those measurements cannot be carried out on the $S_{1.Na}M_{K.SF}$ sample because the fibers obstruct the needle used on the equipment. Nevertheless, these results confirm that the geopolymer mixture must be synthetized with about 10 g of metakaolin M_K in order to optimize the foam stability.

The variations of the surface tension as a function of the surfactant concentration in various geopolymer mixtures are presented in Fig. 8 B, where two different trends can be isolated. In the case of the pure alkaline silicate solution, the addition of a surfactant has no influence on the surface tension which remains constant at around 61 mN.m^{-1}. This phenomenon can be explained by the negative charge of the solution, which remains constant over time because of the nonionic nature of the surfactant. On the other hand, regardless of the geopolymer mixture (with 5 or 10 g of M_K), it is important to note the significant drop in surface tension caused by the addition of the surfactant: a mere 0.1wt% of surfactant leads to a 60% reduction of the surface tension (from 63 to 26 mN.m^{-1} for $^{T(0\%)}S_{1.Na}M_{K(5g)}$ and $^{T(0.1\%)}S_{1.Na}M_{K(5g)}$ respectively). The same behavior is observed for $S_{1.Na}M_{K(10g)}$. From 0.1wt% on, the surface tension value is constant (21 and 20 mN.m^{-1} for $^{T(0.1\%)}S_{1.Na}M_{K(10g)}$ and $^{T(0.2\%)}S_{1.Na}M_{K(10g)}$ respectively). This can be explained by the surfactant absorption at the liquid/air interface, which can modify its properties such as its surface tension [13]. In this case, the shape of the curve is typical of the evolution of the surface tension value with the addition of a surfactant [14, 15]. In the end, this proves that the optimal concentration of surfactant is 0.1wt%.

4. Discussion

The various results obtained on geopolymer foams, and more specifically on the influence of additives, enable the development of a model for a better understanding of the geopolymer foam

formation (Fig. 9).

- Without additives (surfactant and silica fibers), the foam is not stabilized before consolidation. Actually, the reactive mixture has a low viscosity (2.23 Pa.s), thus the gas bubbles formed evolve and tend to escape from the mixture. Besides, a long setting time (115 minutes) leads to the appearance of the coalescence phenomenon. Then, the resulting geopolymer foam exhibits a small porosity rate and a heterogeneous macrostructure.

- The addition of silica fibers causes the increase of the initial viscosity (7.73 Pa.s) but has no influence on the setting time (115 minutes). Thus, the coalescence phenomenon can occur, resulting in the formation of foams with lower porosity and heterogeneous macrostructure with better mechanical properties.

- With the addition of a surfactant, the surface tension of the reactive mixture decreases, with the formation of a tight layer at the liquid-air interface trapping the gas formed within the mixture. However, the setting time remains long; therefore the coarsening phenomenon occurs, leading to a bigger size of the pores and a lower thickness of their walls.

- Finally, the combination of the two additives results in the increase of the initial viscosity, reducing the setting time and the surface tension of the geopolymer mixture. Consequently, the pore size distribution and the thickness of the pore walls are stabilized. As a matter of fact, the decrease of the setting time allows for a faster consolidation of the foam, limiting the coalescence and the coarsening. Ultimately, this enables to synthetize foams with a high porosity and a homogeneous structure, leading to low thermal conductivity characteristics (0.055mW.m^{-1}.K^{-1}).

5. Conclusion

In this work, the influence of additives on geopolymer foam mixtures and therefore on wet foam stabilization was investigated. During the geopolymer foam formation, two difficulties are encountered, (i) the pore formation and its evolution over time and (ii) the geopolymer formation with the polycondensation reaction. This study is based on a formulation in which some additives (filler and/or surfactant) were added.

- Geopolymer foams present different properties depending on the additive used. The addition of a silica filler and a surfactant
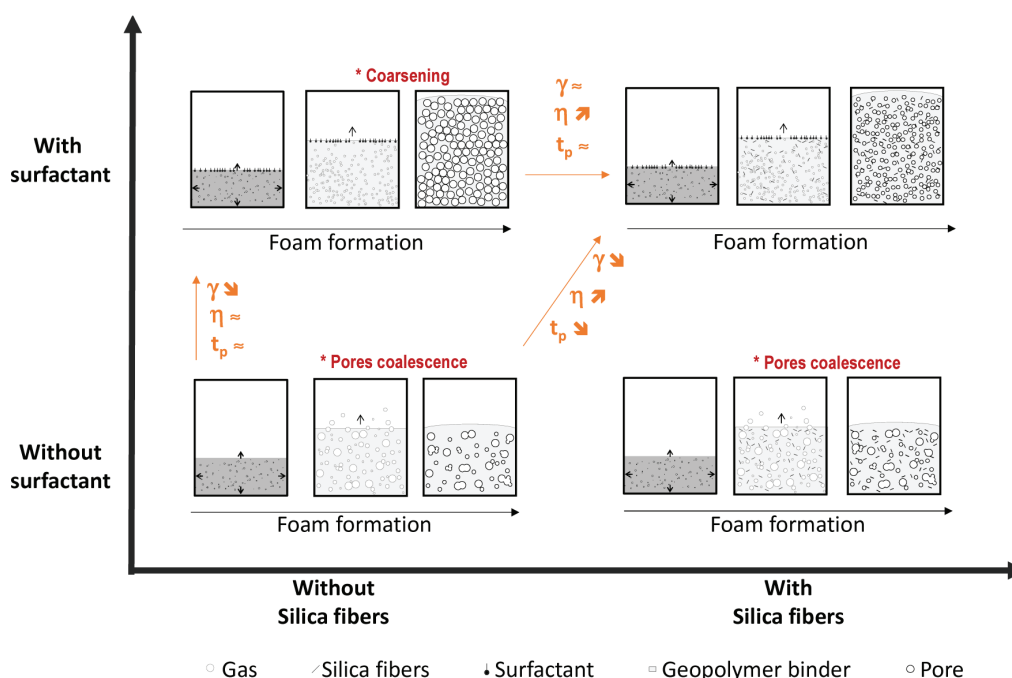

Figure 9. Reactivity model of geopolymer foams with the influence of additives on the porous structure.

leads to the development of foams with a low thermal conductivity (0.057 W.m-1.K-1), a high volume expansion (4.03) and satisfying mechanical properties.

• The FTIR investigation and viscosity analysis reveal that the addition of silica fibers does not have an impact on the geopolymer formation; nevertheless, the use of a surfactant results in the acceleration of the polycondensation reaction.

• The surface tension is highly dependent on the metakaolin content, on the surfactant concentration and on the nature of the medium. By improving the geopolymer mixture inner interactions, adding metakaolin reduces the surface tension. Finally, the surface charge of the medium has a strong influence on the surface tension behavior.

In conclusion, the results presented in this study show that the combine use of a surfactant and fillers in the initial formulation is necessary to control the formation of geopolymer foams.

References

[1] E. Prud'homme, E. Joussein, S. Rossignol, Use of silicon carbide sludge to form porous alkali-activated materials for insulating application, European Physical Journal: Special Topics 224 (2015) 1725-1735.

[2] E. Papa, V. Medri, D. Kpogbemabou, V. Morinière, J. Laumonier, A. Vaccari, S. Rossignol, Porosity and insulating properties of silica-fume based foams, Energy and Buildings 131 (2016) 223-232.

[3] J.L. Provis, J.S.J. van Deventer, Geopolymers. Structure, Processing, Properties and Industrial Applications, Woodhead Publishing Limited (2009).

[4] Z. Zhang, J.L. Provis, A. Reid, H. Wang, Mechanical, thermal insulation, thermal resistance and acoustic absorption properties of geopolymer foam concrete, Cement and Concrete Composites 62 (2015) 97-105.

[5] P. Colombo, M. Griffoni, M. Modesti, Ceramic foams a preceramic polymer and polyurethanes: Preparation and morphological investigations, Journal of Sol-Gel science and technology 13 (1998) 195-199.

[6] D. Weaire, S. Hutzler, The Physics of Foams, Clarendon Press, Oxford (1999).

[7] A. Saint-Jalmes, Physical chemistry in foam drainage and coarsening, Soft Matter 2 (2006) 836-849.

[8] D. Langevin, E. Rio, Coalescence in foams and emulsions, in: P. Somasundaran, Encyclopedia of Surface and Colloid Science, second edition, Taylor and Francis, New York, (2006) 1-15.

[9] I. Cantat, S. Cohen-Addad, F. Elias, F. Graner, R. Hohler, O. Pitois, F. Rouyer, A. Saint-Jalmes, Foams - Structure and Dynamics, Oxford University Press (2013).

[10] P. Stevenson, Foam Engineering: Fundamentals and Applications, Wiley, (2012).

[11] R.J. Pugh, Foaming, foam films, antifoaming and defoaming, Advances in Colloid and Interface Science 64 (1996) 67-142.

[12] M.J. Rosen, Surfactants and Interfacial Phenomena, John Wiley & Sons, Inc (2004).

[13] S. Giasson, Activité de surface : Molécule Amphiphile et Agrégation, PhD thesis, Université de Montréal (2004).

[14] J.W. McBain, Advances Colloid Science, Interscience Publishers, New York (1942) 99.

[15] K.L. Mittal, Micellization Solubilization and microemulsion, New York (1977).

[16] P. Mukerjee, K.J. Mysels, Critical micelle concentrations of aqueous surfactant systems, U.S. National Bureau of Standards, U.S. Govt (1971).

[17] B.M. Folmer, B. Kronberg, Effect of Surfactant-Polymer Association on the Stabilities of Foams and Thin Films:

[18] Sodium Dodecyl Sulfate and Poly(vinyl pyrrolidone), Langmuir 16 (2000) 5987-5992.

[18] S. Cox, D. Weaire, K. Brakke, Liquid foams-precursors for solid foams, Cellular Ceramics: Structure, Manufacturing, Properties and Applications, Wiley (2005).

[19] M. Safouane, M. Durand, A. Saint-Jalmes, V. Bergeron, Aqueous foam drainage. Role of the rheology of the foaming fluid, Journal de. Physique IV 11(2001) 275-280.

[20] S. Bhaskar, G.H. Cho, J.G. Park, S.W. Kim, H.T. Kim, I.J. Kim, Micro porous SiO_2-SiC ceramics from particle stabilized foams by direct foaming, Journal of the ceramic society of Japan 123 (2015) 378-382.

[21] S. Bhaskar, J.G. Park, G.H. Cho, D.N. Seo, I.J. Kim, Influence of SiO_2 content on wet-foam stability for creation of porous ceramics, Journal of the Korean Ceramic Society 51 (2014) 511-515.

[22] T. Wubben, S. Odenbach, Stabilization of liquid metallic foams by solid particles, Colloids and Surfaces A: Physico-chemical and Engineering Aspects 266 (2005) 207-213.

[23] R.H. Ottewill, D.L. Segal, R.C. Watkins, Chemistry & Industry, London, United Kingdom (1981) 57-60.

[24] R.G. Alargova, D.S. Warhadpande, V.N. Paunov, O.D. Velev, Foam superstabilization by polymer microrods, Langmuir 20 (2004) 10371-10374.

[25] J. Henon, A. Alzina, J. Absi, D.S. Smith, S. Rossignol, Potassium geopolymer foams made with silica fume pore forming agent for thermal insulation, Journal of Porous Materials 20 (2013) 37-46.

[26] J. Davidovits, Geopolymer: Chemistry and Application, 2nd ed. Institut Géopolymère, St Quentin (2008).

[27] H. Xu, Geopolymerisation of aluminosilicate materials, PhD thesis, Department of chemical Engineering, University of Melbourne, Australia (2001).

[28] E. Prud'Homme, P. Michaud, E. Joussein, C. Peyratout, A. Smith, S. Arrii-Clacens, J.M. Clacens, S. Rossignol, Silica fume as porogent agent in geo-materials at low temperature, Journal of the European ceramic Society 30 (2010) 1641-1648.

[29] E. Prud'Homme, P. Michaud, E. Joussein, C. Peyratout, A. Smith, S. Rossignol, In situ organic foam prepared from various clays at low temperature, Applied Clay Science 51 (2011) 15-22.

[30] Masson, PEAKOC profile fitting software v1.0, (2006) access at http://www.esrf.eu/Instrumentation/software/data-analysis/OurSoftware/PEAKOC.

[31] A. Gharzouni, E. Joussein, B. Samet, S. Baklouti, S. Rossignol, Effect of the reactivity of alkaline solution and metakaolin on geopolymer formation, Journal of Non-Crystalline Solids 410 (2015) 127-134.

[32] C. Bai, T. Ni, Q. Wang, H. Li, P. Colombo, Porosity, mechanical and insulation properties of geopolymer foams using vegetable oil as the stabilizing agent, Journal of European Ceramic Society 38 (2018) 799-805.

[33] E. Prud'Homme, P. Michaud, E. Joussein, J.M. Clacens, S. Rossignol, Role of alkaline cations and water content on geomaterials foams: monitoring during formation, Journal of non-crystalline solids 357 (2011) 1270-1278.

[34] A. Gharzouni, B. Samet, S. Baklouti, E. Joussein, S. Rossignol, Addition of low reactive clay into metakaolin-based geopolymer formulation: synthesis, existence domains and properties, Powder technology 288 (2016) 212-220.

[35] M. Sakaguchi, I. Sakamoto, R. Akagi, Powder data for potassium sodium silicate $Na_{1.3}K_{0.7}Si_2O_5$, Powder diffraction 10 (1995) 290-292.

[36] K.M.S. Meera, R.M. Sankar, A. Murali, S.N. Jaisankar, A.B. Mandal, Sol-gel network silica/modified montmorillonite clay hybrid nanocomposites for hydrophobic surface coatings, Colloids and surface B: Biointerfaces 90 (2012) 201-210.

[37] H. El-Didamony, I.M. Helmy, Randa M. Osman, A.M.

Habboud, Basalt as Pozzolana and Filler in Ordinary Portland Cement, American Journal of Engineering and Applied sciences 8 (2015) 263-274.

[38] C. Shao, H. Kim, J. Gong, D. Lee, A novel method for making silica nanofibres by using electrospun fibres of polyvinylalcohol/silica composite as precursor, Nanotechnology 13 (2002) 635-637.

[39] E. Prud'Homme, Rôles du cation alcalin et des renforts minéraux et végétaux sur les mécanismes de formation de géopolymères poreux ou denses, PhD thesis, Université de Limoges (2011).

[40] C.A. Rees, J.L. Provis, G.C. Lukey, J.S.J.v. Deventer, Attenuated total reflectance Fourier transform infrared analysis of fly ash geopolymer gel aging, Langmuir, 23 (2007) 8170-8179.

[41] C.A. Rees, J.L. Provis, G.C. Lukey, J.S.J.v. Deventer, In situ ATR-FTIR study of the early stages of fly ash geopolymer gel formation, Langmuir, 23 (2007) 9076-9082.

[42] A. Gharzouni, E. Joussein, B. Samet, S. Baklouti, S. Rossignol, Effect of the reactivity of alkaline solution and metakaolin on geopolymer formation, Journal of non-crystalline solids 410 (2015) 127-134.

[43] A. Gharzouni, I. Sobrados, E. Joussein, S. Baklouti, S. Rossignol, Predictive tools to control the structure and the properties of metakaolin based geopolymer materials,

Colloids and Surfaces A: Physicochemical and Engineering Aspects 511 (2016) 212-221.

[44] J.S.J. van Deventer, J.L. Provis, P. Duxson, G.C. Lukey, Reaction mechanisms in the geopolymeric conversion of inorganic waste to useful products, Journal of Hazardous Materials A139 (2007) 506-513.

[45] S. Jiang, B. Shan, J. Ouyang, W. Zhang, X. Yu, P. Li, B. Han, Rheological properties of cementitious composites with nano/fiber fillers, Construction and Building Materials 158 (2018) 786-800.

[46] P. Overton, E. Danilovtseva, E. Karjalainen, M. Karesoja, V. Annenkov, H. Tenhu, V. Aseyev, Water-Dispersible silica-polyelectrolyte nanocomposites prepared via acid-triggered polycondensation of silicic acid and directed by polycations, Polymers 96 (2016).

[47] G. Giordano, N. Vilà, E. Aubert, J. Ghanbaja, A. Walcarius, Multi-layered, vertically-aligned and functionalized meso-porous silica films generated by sequential electrochemically assisted self-assembly, Electrochimica Acta 237 (2017) 227-236.

[48] L. Vidal, E. Joussein, J. Absi, S. Rossignol, Coating of unreactive and reactive surfaces by aluminosilicate binder, Ceramics International 43 (2017) 1819-182.